JACC: BASIC TO TRANSLATIONAL SCIENCE VOL. 8, NO. 12, 2023
© 2023 THE AUTHORS. PUBLISHED BY ELSEVIER ON BEHALF OF THE AMERICAN COLLEGE OF CARDIOLOGY FOUNDATION. THIS IS AN OPEN ACCESS ARTICLE UNDER THE CC BY-NC-ND LICENSE (http://creativecommons.org/licenses/by-nc-nd/4.0/).

ORIGINAL RESEARCH - PRECLINICAL

TAK1 Activation by NLRP3 Deficiency Confers Cardioprotection Against Pressure Overload-Induced Cardiomyocyte Pyroptosis and Hypertrophy

Xuan Li, PhD,[a,*] Jieyun You, MD, PhD,[b,*] Fangjie Dai, MD, PhD,[a,c,*] Shijun Wang, PhD,[a,*] Feng Hua Yang, PhD,[d] Xingxu Wang, MD, PhD,[b] Zhiwen Ding, PhD,[a] Jiayuan Huang, MD, PhD,[a,d] Liming Chen, MD,[a] Miyesaier Abudureyimu, MD, PhD,[e] Haiyang Tang, PhD,[f,g] Xiangdong Yang, MD, PhD,[a] Yaozu Xiang, MD, PhD,[h] Peter H. Backx, PhD,[i,j] Jun Ren, MD, PhD,[a] Junbo Ge, MD, PhD,[a] Yunzeng Zou, MD, PhD,[a] Jian Wu, MD, PhD[a]

VISUAL ABSTRACT

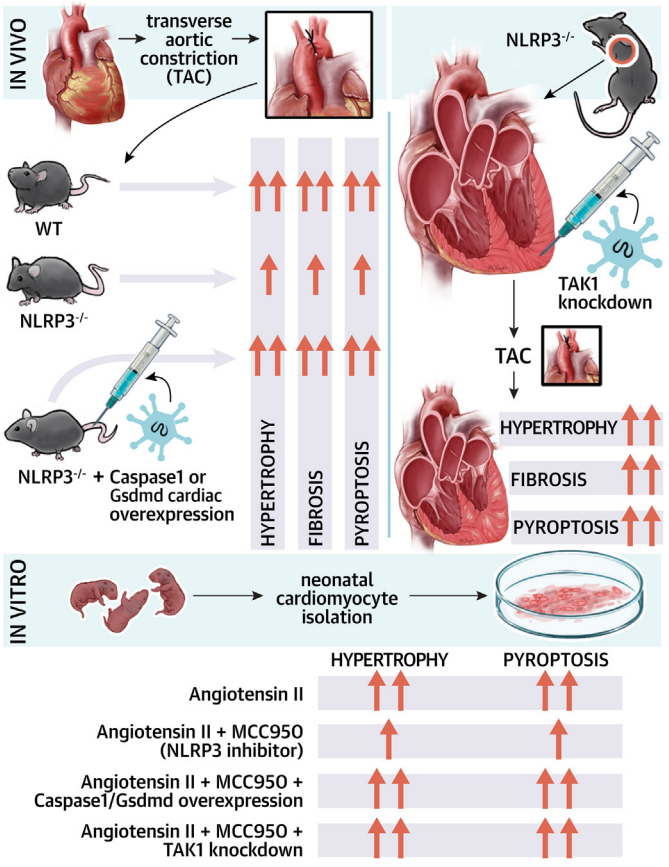

Li X, et al. J Am Coll Cardiol Basic Trans Science. 2023;8(12):1555-1573.

HIGHLIGHTS

- Depression of NLRP3/caspase-1/GSDMD pyroptotic axis attenuates the transition to cardiac dysfunction in pressure overload hearts, whereas either direct or indirect enhancement of the pyroptosis axis accelerates pressure overload-induced heart failure.
- TAK1 activation by NLRP3 deficiency restores pressure overload–induced cardiac hypertrophy and heart failure.
- Reciprocally regulatory role of NLRP3-TAK1 governs pyroptosis and hypertrophy.

ISSN 2452-302X https://doi.org/10.1016/j.jacbts.2023.05.008

JACC: BASIC TO TRANSLATIONAL SCIENCE VOL. 8, NO. 12, 2023
DECEMBER 2023:1555–1573

ABBREVIATIONS AND ACRONYMS

Ang II = angiotensin II

GSDMD = gasdermin D

HW/BW = heart weight-to-body weight ratio

IL = interleukin

KO = knockout

LDH = lactate dehydrogenase

LV = left ventricular

LVEDP = left ventricular end-diastolic pressure

LVEF = left ventricular ejection fraction

LVESP = left ventricular end-systolic pressure

LVFS = left ventricular fractional shortening

LVPWTd = left ventricular posterior wall thickness in end-diastole

LVPWTs = left ventricular posterior wall thickness in end-systole

Max dP/dt = maximal rate of pressure rising

Min dP/dt = maximal rate of pressure fall

NLRP3 = Nod-like receptor (NLR) family pyrin domain containing 3

NMVM = neonatal mouse ventricular myocyte

PBS = phosphate-buffered saline

PCR = polymerase chain reaction

TAC = transverse aortic constriction

TAK1 = transforming growth factor β-activated kinase 1

WT = wild-type

SUMMARY

A comprehensive view of the role of NLRP3/caspase-1/GSDMD–mediated pyroptosis in pressure overload cardiac hypertrophy is presented in this study. Furthermore, mitigation of NLRP3 deficiency-induced pyroptosis confers cardioprotection against pressure overload through activation of TAK1, whereas this salutary effect is abolished by inhibition of TAK1 activity, highlighting a previously unrecognized reciprocally regulatory role of NLRP3-TAK1 governing inflammation-induced cell death and hypertrophic growth. Translationally, this study advocates strategies based on inflammation-induced cell death might be exploited therapeutically in other inflammatory and mechanical overload disorders, such as myocardial infarction and mitral regurgitation. (J Am Coll Cardiol Basic Trans Science 2023;8:1555–1573) © 2023 The Authors. Published by Elsevier on behalf of the American College of Cardiology Foundation. This is an open access article under the CC BY-NC-ND license (http://creativecommons.org/licenses/by-nc-nd/4.0/).

Heart failure is a leading cause of morbidity and mortality worldwide.[1] Left ventricular (LV) hypertrophy not only serves as an adaptive response to adverse stimuli of the heart, but also an independent risk factor for heart failure.[2,3] Pressure overload is considered a primary trigger of compensatory hypertrophic response in the heart.[2] If pressure overload prevails, the heart undergoes a transition from compensated to decompensated cardiac hypertrophy and eventually to heart failure. Mechanisms underlying the transition are rather complicated and remain elusive; recent findings suggest that innate immune activation and sterile inflammation contribute to cell death and ventricular remodeling associated with decompensation.[4-8]

A key component of the innate immune response is Nod-like receptor (NLR) family pyrin domain containing 3 (NLRP3) inflammasome, which is a key pattern-recognition receptor that can be activated to initiate sterile inflammation.[9-11] When activated, NLRP3 turns on pro-caspase-1 to generate cleaved caspase-1.[12] In addition to the secretion of proinflammatory cytokines interleukin (IL)-1β and interleukin (IL)-18, activated caspase-1 also triggers the cleavage of gasdermin D (GSDMD), an executor of pyroptosis, a proinflammatory form of programmed necrosis.[13] NLRP3/caspase-1/GSDMD-mediated pyroptosis was first identified in monocytes and macrophages, and was only recently detected in other types of cells such as cardiomyocytes.[14,15] It is worth noting the cell-type-specific roles of NLRP3 wherein it fuels pyroptosis by releasing both IL-18 and IL-1β in cardiac fibroblasts, while only releasing IL-18 in cardiomyocytes.[16,17] It is apparent that cardiac sterile inflammation is effectively triggered by cell death and contributes to heart failure in ischemic heart disease,[18] and several heart failure trials are exploring the efficacy of therapeutic targeting NLRP3, with some promising preliminary results.[19,20] More recent animal studies have suggested that cardiac inflammation also plays an important role in nonischemic heart disease[5,21] with pressure overload inducing inflammatory responses that are distinct from cell

From the [a]Shanghai Institute of Cardiovascular Diseases, Zhongshan Hospital and Institutes of Biomedical Sciences, Fudan University, Shanghai, China; [b]Department of Cardiovascular Medicine, Shanghai East Hospital, School of Medicine, Tongji University, Shanghai, China; [c]Department of Cardiology, Affiliated Hospital of Guizhou Medical University, Guiyang, China; [d]Guangdong Laboratory Animals Monitoring Institute, Guangdong Province Key Laboratory of Laboratory Animals, Guangzhou, China; [e]Cardiovascular Department, Shanghai Xuhui Central Hospital, Fudan University, Shanghai, China; [f]State Key Laboratory of Respiratory Disease, National Clinical Research Center for Respiratory Disease, Guangzhou, China; [g]Guangdong Key Laboratory of Vascular Disease, Guangzhou Institute of Respiratory Health, The First Affiliated Hospital of Guangzhou Medical University, Guangzhou, China; [h]Shanghai East Hospital, Key Laboratory of Arrhythmias of the Ministry of Education of China, School of Life Sciences and Technology, Tongji University, Shanghai, China; [i]Department of Biology, Faculty of Science, York University, Toronto, Ontario, Canada; and the [j]Toronto General Research Institute, University Health Network, Toronto, Ontario, Canada.
*Drs Li, You, Dai, and S. Wang contributed equally to this work as first authors.
The authors attest they are in compliance with human studies committees and animal welfare regulations of the authors' institutions and Food and Drug Administration guidelines, including patient consent where appropriate. For more information, visit the Author Center.

Manuscript received February 7, 2023; revised manuscript received May 16, 2023, accepted May 16, 2023.

death responses in ischemic heart disease.[18] Moreover, although numerous studies have demonstrated marked protection against myocardial injury resulting from myocardial infarction or ischemia-reperfusion by NLRP3 inhibition,[22] the efficacy of NLRP3 inhibition remains controversial in pressure overload-induced cardiac hypertrophy, with several lines of evidence showing contradictory results.[23-25]

Transforming growth factor β-activated kinase 1 (TAK1) is pivotal for regulating important physiological processes, including immune cell activation, inflammation, and cardiac hypertrophic response.[26] A recent study has reported that TAK1 restricts NLRP3 activation and cell death to control myeloid proliferation, whereas absence of TAK1 in macrophages induces NLRP3 activation.[27] Very recently, it is reported that blockade of TAK1 leads to cytotoxicity with the hallmarks of GSDMD cleavage and pyroptosis.[28] Nevertheless, it remains enigmatic that although activation of TAK1 induces cardiac hypertrophy at baseline or in response to pressure overload,[29,30] deficiency of TAK1 induces cell death and cardiac dysfunction.[26] Therefore, we hypothesized that the NLRP3/caspase-1/GSDMD axis through its closely relevant signaling effectors fine tunes the disparate effects of pyroptosis and hypertrophic response in pressure overload hearts. In the present study, we demonstrated that NLRP3 deficiency attenuated myocardial pyroptosis and preserved cardiac function under pressure overload, whereas direct or indirect enhancement of pyroptosis abrogated the compensation. Moreover, down-regulation of TAK1 abolished the cardioprotection of NLRP3 deficiency due to the causative imbalance of pyroptosis and hypertrophic growth.

METHODS

MICE AND GENETIC MANIPULATIONS. The animal experiments were approved by the animal care and use committee of Zhongshan Hospital, Fudan University, and procedures were performed in accordance with National Institutes of Health Guide for the Care and Use of Laboratory Animals (NIH Publication No. 85-23, Revised 2011). NLRP3-knockout (KO, $^{-/-}$) mice (C57BL/6J background) were obtained from the Jackson Laboratory (stock number: 021302). Male NLRP3 KO mice and their wild-type (WT) littermates (aged 9 to 12 weeks) were subjected to transverse aortic constriction (TAC) surgery to investigate the effect of NLRP3 deficiency on cardiac hypertrophy. For the genotyping of NLRP3 KO mice, the toes of 2-week-old mice were clipped for DNA extraction and identified by polymerase chain reaction (PCR) using a One Step Mouse Genotyping Kit (No. PD101-01, Vazyme). The forward primer TCAGTTTCCTTGGCTACCAGA, the WT reverse primer TTCCATTACAGTCACTCCAGATGT, and the mutant reverse primer TGCCTGCTCTTTACTGAAGG were used for the genotyping of *NLRP3*$^{-/-}$ mice. The WT allele yielded a band of 666 bp, and the NLRP3 knockout allele yielded a band of 850 bp. To specifically overexpress caspase-1 or GSDMD in the myocardium, mice were administered a tail vein injection of adeno-associated virus type 9 (AAV9) vector carrying recombinant caspase-1 (pAOV-cTNT-EGFP-2A-Casp1-3Flag, Obio Biotechnology, hereafter stated as Oe-caspase-1) or GSDMD (pAOV-cTNT-EGFP-2A-Gsdmd-3Flag, Obio Biotechnology, hereafter stated as Oe-GSDMD), respectively, with the cardiac troponin T (cTnT) promoter. Vector virus AAV9-EGFP (pAOV-cTNT-EGFP-2A-MCS-3Flag, Obio Biotechnology, hereafter stated as EGFP) was used as a negative control. To specifically knockdown TAK1 in the myocardium, mice were administered an ultrasound-guided closed-chest intramyocardial injection of AAV9 carrying small hairpin RNA against TAK1 (pLKD-CMV-G&PR-U6-Map3k7 shRNA, Obio Biotechnology, hereafter stated as shTAK1), in line with its corresponding negative control (pLKD-CMV-G&PR-U6-shRNA, Obio Biotechnology, hereafter stated as shRNA). A total of 1×10^{11} viral particles were injected into mice 3 weeks before TAC surgery. The infection efficiency of the aforementioned virus was evaluated by fluorescence detection 3 weeks after injection, or by Western blot at the end point of experiments. Only male mice were enrolled in this study to minimize variability between groups. All mice were housed under controlled conditions (24°C ± 2°C, 12:12-hour light-dark cycle, and chow and water ad libitum).

TAC SURGERY. TAC surgery was performed to induce cardiac pressure overload in mice as we described previously.[31,32] In brief, under 2% isoflurane, the trachea was intubated and connected to a ventilator, the left chest was disinfected and opened up through the second intercostal space, and the aorta between the innominate artery and the left common carotid artery was isolated and then constricted using a 6-0 silk thread tied to a blunt 27-gauge needle, which was carefully pulled out to form an aortic constriction. After the skin of mice was sutured with 4-0 silk thread and disinfected, meloxicam (0.13 mg) was administered for analgesia. Sham mice underwent a similar operation without banding of the aorta.

ECHOCARDIOGRAPHY. Echocardiographic assessment was assessed using a Vevo2100 high-frequency ultrasound system with a 30 MHz probe

(VisualSonics). Good intra- and interobserver agreement on echocardiographic results was indicated in our hands.[33-36] In brief, mice were anesthetized in 1.5% isoflurane, positioned on a heating pad to maintain normothermia, heart rate was maintained at around 500 beats/min, and the M-mode of the LV structure and function was evaluated at the papillary muscle level in the parasternal long-axis view. The following indices were acquired: LV posterior wall thickness in end-diastole (LVPWTd) and end-systole (LVPWTs), and LV ejection fraction (LVEF) and fractional shortening (LVFS). The probe was then placed on the right side of the chest and tilted horizontally to show the aortic arch, the color Doppler mode and pulse-wave Doppler mode were applied, the Doppler intercept angle between the ultrasound direction and blood flow direction was controlled within 20°, and the peak systolic velocity of aortic arch flow was acquired to indicate the adequacy of aortic constriction. Peak flow velocity at the banding site ≥3.5 m/s was considered successful in TAC establishment and underwent further analysis.[32,37,38]

INVASIVE HEMODYNAMICS. LV performance was further evaluated by invasive hemodynamic measurement using the Power Laboratory system (AD Instruments) with a 1.4-F micromanometric catheter (SPR 835, Millar Instruments) as we previously described.[35,38] Under stable anesthesia with 1.5% isoflurane, mice were placed in a supine position, a longitudinal incision (around 1 cm) was made in the middle of cervical area, the right common carotid artery was isolated, and the micromanometer was inserted into the artery and carefully advanced into the LV. LV end-systolic pressure (LVESP) and end-diastolic pressure (LVEDP) were acquired for evaluation of LV pressure, whereas maximal rate of pressure rising (Max dP/dt) and maximal rate of pressure fall (Min dP/dt) were derived for evaluation of LV systolic and diastolic function, respectively.

HISTOLOGICAL ANALYSIS. After collection of invasive hemodynamic data, mice were euthanized by cervical dislocation under 4% isoflurane. The hearts were excised, rinsed in saline, dried on filter paper, then heart weights and heart weight-to-body weight ratio (HW/BW) were measured. The hearts were then fixed in 10% formalin, embedded in paraffin, and sectioned transversely to a 4-μm thickness at the papillary muscle level symbolized by the most expansive part of the heart. The slides were then stained with hematoxylin and eosin for evaluation of cardiomyocyte size, or with Masson trichrome for interstitial fibrosis and perivascular fibrosis. Digital photographs were acquired by the Qwin V3 optical microscope system (Leica), at a magnification of ×400 times for myocyte size and ×200 for fibrosis. With the help of an image analysis software (Image-Pro Plus 5.0, Media Cybernetics,), cross-sectional areas of LV cardiomyocytes were measured, and the degree of fibrosis was expressed as the ratio of Masson trichrome-stained area to total LV area.

REAL-TIME QUANTITATIVE PCR. Total RNA was isolated from LV heart tissue or treated cardiomyocytes using TRIZOL reagent. cDNA was synthesized using the PrimeScript 1st Strand DNA Synthesis Kit (Takara). Real-time quantitative PCR was performed on an ABI 7500 real-time PCR System (Applied Biosystems) using SYBR Premix Ex Taq II (Takara) with primers listed in Supplemental Table 1. Expression levels of target genes were shown as $2^{-\Delta\Delta Ct}$ of the target gene relative to glyceraldehyde-3-phosphate dehydrogenase (GAPDH).

WESTERN BLOT. Total proteins were obtained from LV heart tissue or treated cells. Electrophoresis for protein (20 to 40 μg) was performed by 10% or 12.5% SDS-polyacrylamide gel and then proteins were transferred to 0.22-μm PVDF membrane (Millipore). After blocking with 5% bovine serum albumin for 2 hours at room temperature, PVDF membrane with target protein was sequentially incubated with primary antibodies overnight at 4°C and secondary antibodies for 2 hours at room temperature. The primary antibodies and secondary antibodies used for Western blot analysis are listed in Supplemental Table 2. Afterwards, the imprint on the PVDF membrane treated by a Millipore ECL kit (Invitrogen) was detected by Western blot detection system (Bio-Rad), and the optical density of target protein was quantified using ImageJ analysis software (1.52v, National Institutes of Health).

STRING AND CYTOSCAPE INTEGRATIVE NETWORK ANALYSIS. Protein-protein interactions between NLRP3 and TAK1 were retrieved from STRING (version 11.5) for humans with medium confidence score and experimentally validated from Cytoscape (version 3.9.1) to construct interaction networks.[39,40]

STRUCTURE-BASED PROTEIN INTERACTION INTERFACE ANALYSIS BETWEEN NLRP3 AND TAK1. The protein structure of NLRP3 was predicted by template-based homology structure modeling tool SWISS-MODEL, using the NLRP3 structure as the template (Protein Data Bank (PDB) ID: 6NPY, chain A). The experimental

structure of TAK1 was downloaded from the PDB database (PDB ID: 3P0U, Chain A). Structures of proteins were submitted to the PRISM tool to predict their potential interaction interface.[41]

COIMMUNOPRECIPITATION ASSAY. Proteins were extracted from cultured cardiomyocytes or cardiac tissue and incubated with primary antibodies at 4°C overnight. The antibodies used in this study were as follows: anti-IgG (Cell Signaling Technology, #3900, 1:200), anti-NLRP3 (Cell Signaling Technology, #15101, 1:200, or Abcam, #ab263899, 1:30), and anti-HA (Proteintech, Cat No. 51064-2-AP, 1:100). The mixture was then incubated with 30 μL of Protein A/G Agarose Resin (YEASEN, #36403ES03) for 2 hours with rotation. After eluting the surface nonspecific binding, samples were obtained from the resin-antibody complexes and subjected to immunoblot.

HL-1 CELL CULTURE AND PLASMID TRANSFECTION. Murine cardiomyocytes cell line (HL-1 cells) was purchased from Sigma-Aldrich (#SCC065) and cultured in DMEM medium supplemented with 10% fetal bovine serum. Murine HA-tagged WT NLRP3 plasmids, murine Flag-tagged WT TAK1, and the S412A mutation plasmids were purchased from Hanbio Co., Ltd. Plasmids were transfected with Hieff TransTM Liposomal Transfection Reagent (YEASEN, #40802ES02) following the manufacturer's protocol.

PRIMARY NEONATAL MOUSE VENTRICULAR MYOCYTES CULTURE, ADENOVIRUS TRANSFECTION, AND IMMUNOFLUORESCENCE STAINING. Primary neonatal mouse ventricular myocytes (NMVMs) were isolated from 1- to 3-day-old C57BL/6J mice and cultured as previously described.[42] Briefly, hearts were cut into 1-mm^3 pieces and digested in 0.08% collagenase 1 (Worthington) at 37°C. The supernatant was then collected and neutralized with complete medium (DMEM/F12 culture medium containing 10% fetal bovine serum). After repeating these steps 6 to 8 times, all the collected supernatant was filtered through a 70-μm filter and centrifuged at 1,000 rpm for 5 minutes. The cell pellets were resuspended in complete medium and plated onto 10-cm culture dishes for 1 to 2 hours. The supernatant was then collected and plated on culture dishes for further experiments.

After being plated for 24 hours, the complete medium was replaced by serum-free medium for 12 hours, then cardiomyocytes were exposed to angiotensin II (Ang II) (1 μmol/L), MCC950 (10 μmol/L), or a combination of both in fresh serum-free medium for another 48 hours. For adenovirus infection, before the replacement of complete medium to serum-free medium and exposure to Ang II (1 μmol/L) or MCC950 (10 μmol/L), cardiomyocytes were infected with adenovirus for 8 hours, then cultured for 48 hours. The CASPASE1-overexpressing adenovirus (pAdeno-EF1A(S)-mNeonGreen-CMV-Casp1-3FLAG), GSDMD-overexpressing adenovirus (pAdeno-EF1A(S)-mNeonGreen-CMV-Gsdmd-3FLAG), TAK1 shRNA adenovirus (pDKD-CMV-eGFP-U6-shRNA (Map3k7)), and negative control (Ad-control) were purchased from Obio Technology (Shanghai, China).

For immunofluorescence staining, after culture medium was removed, cardiomyocytes were rinsed with phosphate-buffered saline (PBS) 3 times and fixed with 4% paraformaldehyde for 15 minutes, permeabilized with 0.5% Triton X-100 in PBS for 5 minutes, and saturated with 5% bovine serum albumin in PBS at room temperature for 1 hour. Cardiomyocytes then were incubated with cTnT (Abcam, #ab8295, 1:200) antibodies overnight at 4°C. After being rinsed with PBS 3 times, cardiomyocytes were incubated with IgG H&L (Alexa Fluor 594, Abcam, #ab150076, 1:500) for 1 hour at room temperature. After incubation with Antifade Mounting Medium with DAPI (Beyotime, P0131-25ml) for 5 minutes, cardiomyocytes were examined under a fluorescence microscope, and cross-sectional areas of cardiomyocytes were calculated by ImageJ software (1.48v).

LACTATE DEHYDROGENASE MEASUREMENT. Cardiomyocyte supernatants were collected and tested for lactate dehydrogenase (LDH) level with an LDH Cytotoxicity Assay Kit (Beyotime) according to the manufacturer's instructions.

STATISTICAL ANALYSIS. All continuous data in this study are presented as the mean ± SEM. GraphPad Prism 8 (GraphPad Software) was used for statistical analysis. Normality of the data was assessed by the Shapiro-Wilk test, and all continuous data met the normal distribution assumption. The difference between 2 groups was analyzed by 2-tailed Student's *t*-tests, and the difference among multiple groups was analyzed by 2-way analysis of variance (surgery and genetic background), followed by Student-Newman-Keuls correction for post hoc multiple pairwise comparisons. A P value <0.05 was considered statistically significant.

RESULTS

DEFICIENCY OF NLRP3 ATTENUATES MYOCARDIAL PYROPTOSIS AND CARDIAC HYPERTROPHY IN PRESSURE OVERLOAD HEARTS. In order to examine further the controversial role of NLRP3 deficiency in pressure overload-induced cardiac remodeling,[11,18,23,24] WT mice and NLRP3 KO mice (Supplemental Figure 1) were subjected to TAC. After 2 weeks of TAC, both groups of

FIGURE 1 **NLRP3 Deficiency Attenuates Left Ventricular Dilation and Preserves Cardiac Function in Pressure Overload Hearts**

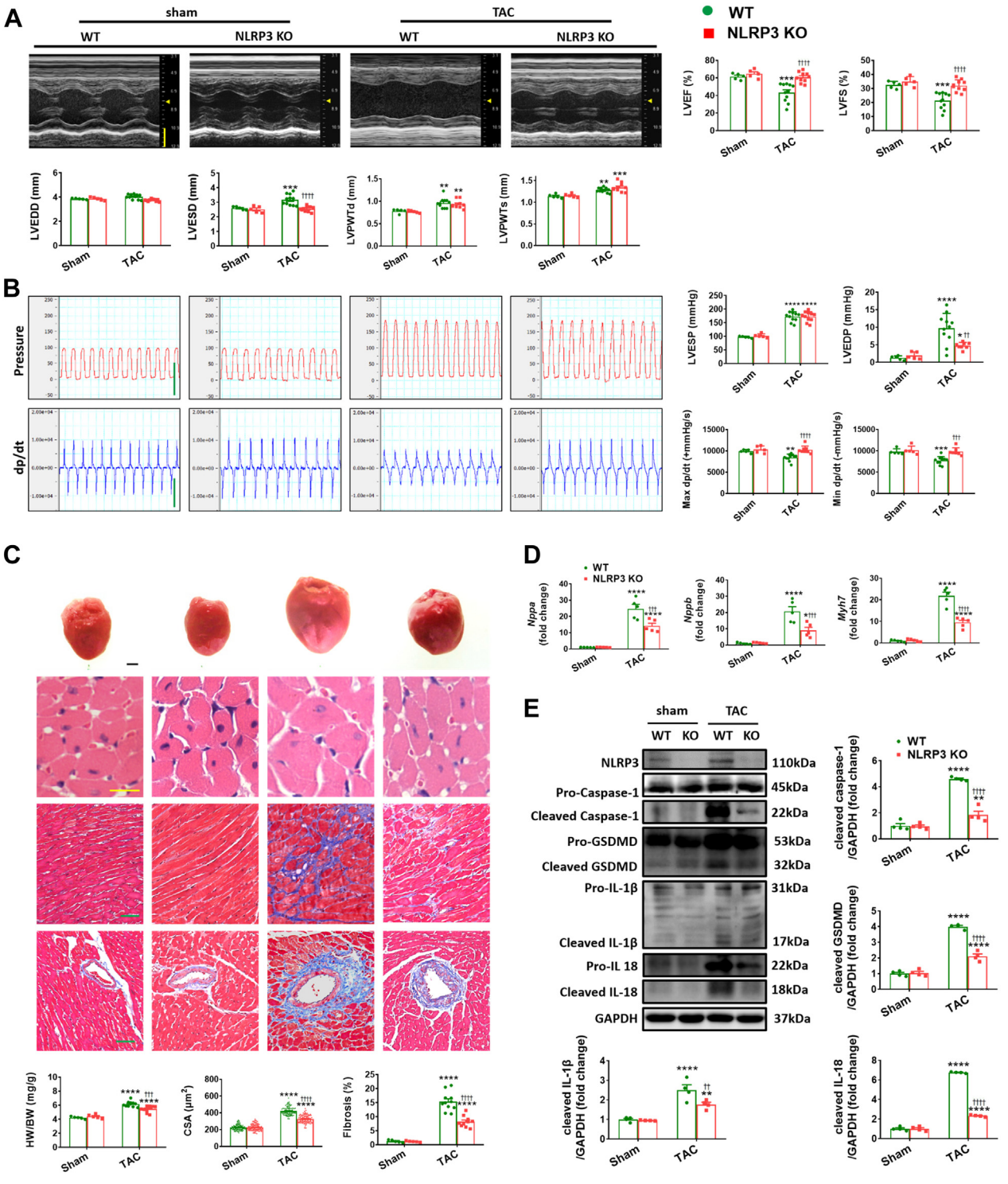

Continued on the next page

mice showed preserved cardiac function featuring adaptive hypertrophy (Supplemental Table 3). After 4 weeks of TAC, WT mice displayed marked cardiac dysfunction (as evidenced by compromised LVEF, LVFS, Max dp/dt, and Min dp/dt, in line with elevated LVEDP) (**Figures 1A and 1B**, Supplemental Table 4), whereas NLRP3 KO mice displayed far better cardiac function (**Figure 1B**, Supplemental Figure 2) despite similar pressure overload between the groups (as assessed by peak systolic velocity of aortic arch flow and LVESP measurements) (**Figure 1B**). Consistent with the functional improvement, the loss of NLRP3 also protected mice from TAC-induced adverse tissue remodeling as evidenced by marked reductions in fibrosis (**Figure 1C**) and the expression of markers of hypertrophy (*Nppa*, *Nppb*, and *Myh7*) (**Figure 1D**) accompanied by more modest improvements in HW/BW, inner dimension, wall thickness, and cardiomyocyte size in response to 4 weeks of TAC compared with WT mice (**Figures 1A and 1C**). Importantly, the absence of NLRP3 blunted profoundly the elevations in cleaved caspase-1, cleaved IL-18, and cleaved IL-1β seen in WT mice after 4 weeks of TAC (**Figure 1E**) and this was accompanied by marked reductions in the extent of induction of the pyroptosis executor and marker (cleaved) GSDMD levels seen in TAC WT mice (**Figure 1E**).

To further assess the role of NLRP3 activation in hypertrophic myocardium, we treated NMVMs with Ang II for 48 hours with or without MCC950 (a selective inhibitor of NLRP3). As expected, Ang II treatment induced marked cardiomyocyte hypertrophy along with up-regulation of hypertrophy markers *Nppa*, *Nppb*, and *Myh7* (Supplemental Figures 3A and 3B) compared with PBS-treated cultures. Not only did MCC950 suppress the extent of Ang II-mediated hypertrophy, but it also largely ameliorated cleavage of caspase-1 as well as the elevated levels of IL-18 and GSDMD induced by Ang II (Supplemental Figures 3A and 3C). IL-1β was not assessed in these studies because previous studies have demonstrated that cardiomyocytes do not express and secrete IL-1β in similar culture conditions.[17,43,44] In addition, Ang II treatment caused notable destruction of cell membrane integrity as assessed by LDH level, whereas MCC950 administration reduced the LDH level in the supernatant of Ang II-treated NMVMs (Supplemental Figure 4A). Thus, both in vivo and in vitro results indicate that NLRP3 deficiency restores cardiac dysfunction and mitigates cardiac pyroptosis and remodeling under pressure overload.

INDIRECT UP-REGULATION OF PYROPTOSIS BY CASPASE-1 OVEREXPRESSION ABROGATES THE CARDIOPROTECTION CONFERRED BY NLRP3 DEFICIENCY. Because NLRP3 inflammasome activation involves caspase-1 cleavage/activation, which in turn cleaves and activates GSDMD to initiate pyroptosis,[12] we overexpressed caspase-1 (or GFP for controls) in the myocardium through intravenous injection of AAV9 carrying caspase-1 with the cTnT promotor. Robust infection efficiency was confirmed either by fluorescence levels or by expression levels of caspase-1 Western blot at the end point of experiments (**Figures 2A and 2B**, Supplemental Figures 5A). Although AAV9-induced caspase-1 overexpression had no effect on pyroptosis at baseline, it did lead to a resurgence of pyroptosis in NLRP3 KO mice challenged with pressure overload, as evidenced by enhanced cleaved GSDMD, cleaved IL-18, and cleaved IL-1β (**Figure 2B**). Moreover, after caspase-1 overexpression, TAC induced progressive decompensation of cardiac function in NLRP3 KO as indicated by decreased LVEF, LVFS, Max dp/dt, and Min dp/dt, increased LVEDP, HW/BW,

FIGURE 1 Continued

(A) Representative M-mode echocardiograms and relevant quantification of left ventricle in wild-type (WT) or NLRP3 knockout (KO) mice 4 weeks after transverse aortic constriction (TAC) or sham operation (n = 5 to 11 mice per group). Vertical scale bar, 2 mm, horizontal scale bar, 0.1 seconds. (B) Schematic presentations and quantification of left ventricular pressure, schematic presentations and quantification of left ventricular contraction velocity and relaxation velocity (n = 5 to 11 mice per group). Vertical scale bar, 100 mm Hg/s for pressure, 10,000 mm Hg/s for dp/dt; horizontal scale bar, 0.5 seconds for pressure and dp/dt. (C) Upper to lower, representative images of heart, cardiomyocytes stained by hematoxylin and eosin (scale bar, 20 μm), interstitial fibrosis stained by Masson's trichrome (scale bar, 50 μm), perivascular fibrosis stained by Masson's trichrome (scale bar, 50 μm), quantification of heart weight to body weight ratio (HW/BW), cross-sectional areas (CSA) of cardiomyocyte (n = 100 cells per group), and fibrotic ratio expressed as % area (n = 10 to 22 fields per group). (D) Real-time quantitative polymerase chain reaction (PCR) analyses for the mRNA levels of atrial natriuretic peptide (*Nppa*), brain natriuretic peptide (*Nppb*), and beta-myosin heavy chain (*Myh7*) in left ventricular samples (n = 4 independent experiments). (E) Representative Western blot images and quantification showing NLRP3 and the cleaved- and pro-forms of caspase-1, GSDMD, IL-1β, and IL-18 in left ventricular samples (n = 4 independent experiments). Mean ± SEM. *$P < 0.05$, **$P < 0.01$, ***$P < 0.001$, ****$P < 0.0001$ vs sham, ††$P < 0.01$, †††$P < 0.001$, ††††$P < 0.0001$ vs WT. LVEF = left ventricular ejection fraction; LVEDD = left ventricular end-diastolic dimension; LVEDP = left ventricular end-diastolic pressure; LVESD = left ventricular end-systolic dimension; LVESP = left ventricular end-systolic pressure; LVFS = left ventricular fractional shortening; LVPWTd = left ventricular posterior wall end-diastolic thickness; LVPWTs = left ventricular posterior wall end-systolic thickness; Max +dp/dt = maximal rate of rise in left ventricular pressure; Min −dp/dt = maximal rate of fall on left ventricular pressure.

FIGURE 2 Caspase-1 Mediated Aggravation of Pyroptosis Abrogates the Cardioprotection Conferred by NLRP3 Deficiency Under Pressure Overload

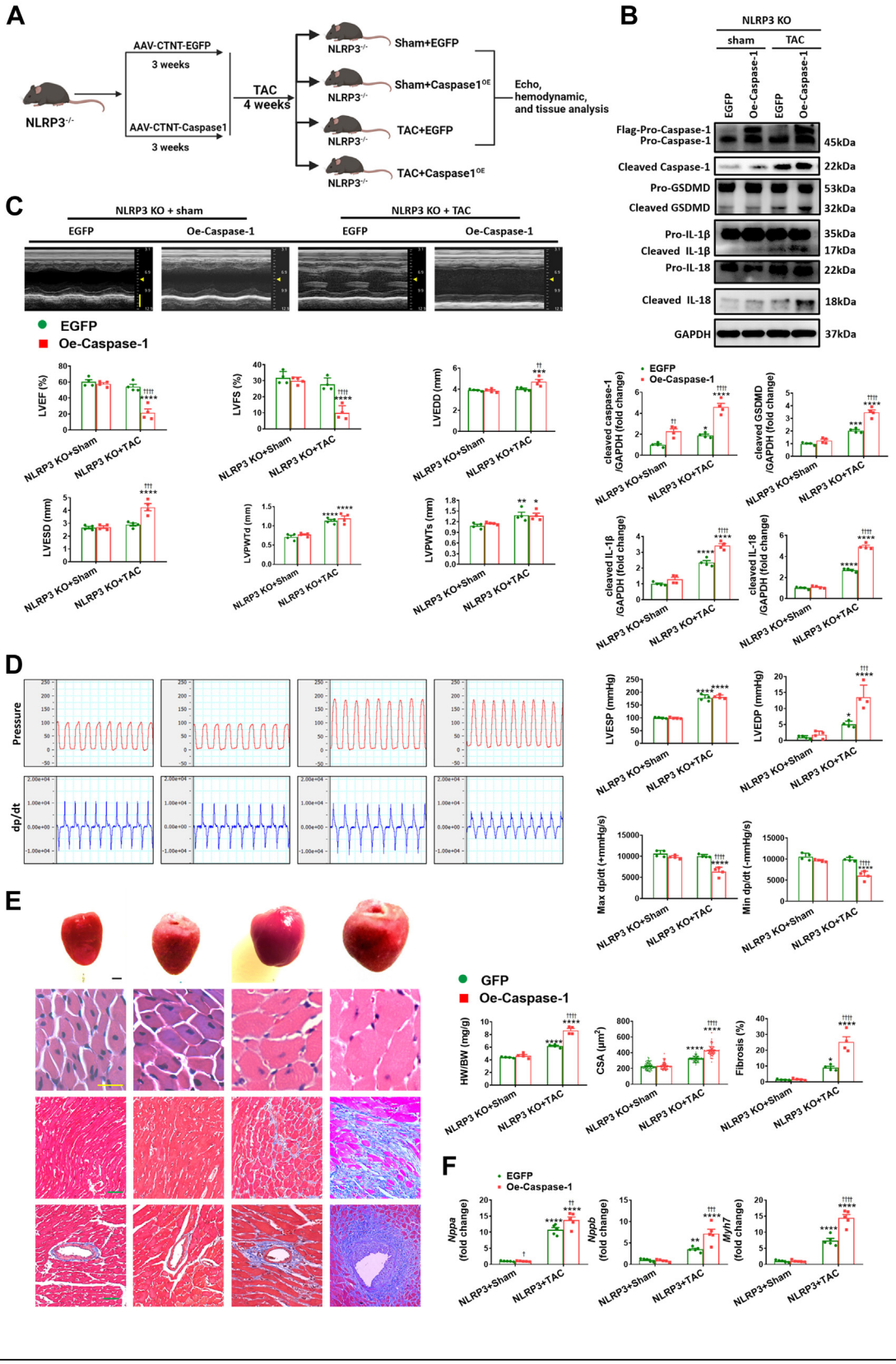

Continued on the next page

inner dimension, wall thickness, cardiomyocyte size, and fibrosis, and the reactivation of the fetal genes *Nppa*, *Nppb*, and *Myh7* (**Figures 2C to 2F**, Supplemental Table 5). Consistent with the in vivo findings, caspase-1 overexpression in cardiomyocytes (Supplemental Figure 6) eliminated the ability of MCC950 to protect NMVMs against the Ang II–mediated hypertrophic responses and the activation of pyroptosis-related signaling pathways (Supplemental Figure 7) as well as LDH release (Supplemental Figure 4B). Collectively, these results indicate that indirect up-regulation of pyroptosis remarkably blunts the cardioprotection conferred by NLRP3 deficiency.

DIRECT UP-REGULATION OF PYROPTOSIS BY GSDMD OVEREXPRESSION ABOLISHES THE BENEFICIAL EFFECTS OF NLRP3 DEFICIENCY. To explore more directly the role of GSDMD in pyroptosis, we also overexpressed GSDMD in the myocardium using AAV9 (**Figures 3A and 3B**, Supplemental Figure 5B). Following GSDMD overexpression, pressure overload now induced elevations in IL-18 and cleaved IL-1β (**Figure 3B**) in heart lacking NLRP3, whereas it had no effect on these mice following sham operation. Correspondingly, GSDMD overexpression in NLRP3-null mice transitioned from compensated hypertrophy to decompensated hypertrophy following TAC, as indicated by decreased LVEF, LVFS, Max dp/dt, and Min dp/dt, increased LVEDP, HW/BW, inner dimension, wall thickness, cardiomyocyte size, and fibrosis, and enhanced reprogramming of fetal genes *Nppa*, *Nppb*, and *Myh7* (**Figures 3C to 3F**, Supplemental Table 6). In agreement with the in vivo findings, GSDMD overexpression (Supplemental Figure 6B) not only recapitulated the pyroptosis-related signaling and LDH release (Supplemental Figure 4C), but also greatly regressed the hypertrophy-reducing effects of MCC950 in NMVMs, as indicated by enlarged cardiomyocyte size and enhanced expression of hypertrophic markers (Supplemental Figure 8).

Given that other NLR family members, such as NLRP1 (NLR family pyrin domain containing 1) and NLRC4 (NLR family CARD domain containing 4), also recruit and activate caspase-1,[12,45,46] we examined the alterations of NLRP1 and NLRC4 to interrogate whether the detrimental effect exerted by overexpression of exogenous caspase-1 and GSDMD under pressure overload in the absence of NLRP3 may be attributed to NLRP1 or NLRC4. Our results demonstrate that both NLRP1 and NLRC4 are up-regulated in NLRP3 KO mice under pressure overload in relative to corresponding sham-operated mice (Supplemental Figure 9).

NLRP3 DEFICIENCY ENHANCED ACTIVATION LEVELS OF TAK1 IN HYPERTROPHIC HEARTS. The aforementioned results support the conclusion that NLRP3/caspase-1/GSDMD signaling contributes importantly to adverse hypertrophic remodeling in response to chronic pressure overload. We next sought to assess the connection between NLRP3 and other signaling pathways implicated in cardiac hypertrophy. One such pathway is Akt, which is critical in physiological hypertrophy.[34,47] However, inhibition of phosphoinositide 3-kinase (PI3K)-Akt signaling using Wortmannin[34,48] had no effect on responses to TAC of hearts lacking NLRP3 (Supplemental Figure 10), implying that Akt activation is dispensable for the protection against pressure overload observed following NLRP3 ablation. Another possible hypertrophic candidate is TAK1, which is an

FIGURE 2 Continued

(A) In vivo experimental overall schematic to explore the effects of cardiac caspase-1 overexpression in NLRP3 KO mice subjected to TAC. Male NLRP3 KO mice were administered a tail vein injection of adeno-associated virus type 9 (AAV9) vector carrying recombinant caspase-1, with the cardiac troponin T (cTnT) promoter. Vector virus AAV9-EGFP was used as negative control. Three weeks later, these mice were subjected to TAC surgery or sham operation for 4 weeks, followed by echo, hemodynamic, and tissue analysis. (B) Representative Western blot images and quantification showing the cleaved- and pro-forms of caspase-1, GSDMD, IL-1β, and IL-18 in left ventricular samples from NLRP3 KO mice with AAV9 transfected caspase-1 (Oe-caspase-1) or enhanced green fluorescent protein (EGFP) after 4 weeks of TAC or sham operation (n = 4 independent experiments). (C) Representative M-mode echocardiograms and quantification of left ventricle (n = 4 mice per group). Vertical scale bar, 2 mm, horizontal scale bar, 0.1 second. (D) Schematic presentations and quantification of left ventricular pressure, schematic presentations and quantification of left ventricular contraction velocity and relaxation velocity (n=4 mice per group). Vertical scale bars, 100 mm Hg/s for pressure, 10,000 mm Hg/s for dp/dt; horizontal scale bar, 0.5 second for pressure and dp/dt. (E) Upper to lower, representative images of heart, cardiomyocytes stained by hematoxylin and eosin (scale bar, 20 μm), interstitial fibrosis stained by Masson's trichrome (scale bar, 50 μm), perivascular fibrosis stained by Masson's trichrome (scale bar, 50 μm), quantification of HW/BW, CSA of cardiomyocyte (n = 100 cells per group), and fibrotic ratio expressed as % area (n = 8 to 10 fields per group). (F) Real-time quantitative PCR analyses for the mRNA levels of atrial natriuretic peptide (*Nppa*), brain natriuretic peptide (*Nppb*), and beta-myosin heavy chain (*Myh7*) in left ventricular samples (n = 4 independent experiments). Mean ± SEM. *$P < 0.05$, **$P < 0.01$, ***$P < 0.001$, ****$P < 0.0001$ vs sham, ††$P < 0.01$, †††$P < 0.001$, ††††$P < 0.0001$ vs EGFP. Abbreviations as in **Figure 1**.

FIGURE 3 GSDMD Execution of Pyroptosis Decompensates Cardiac Function in NLRP3 Deficiency Mice Under Pressure Overload

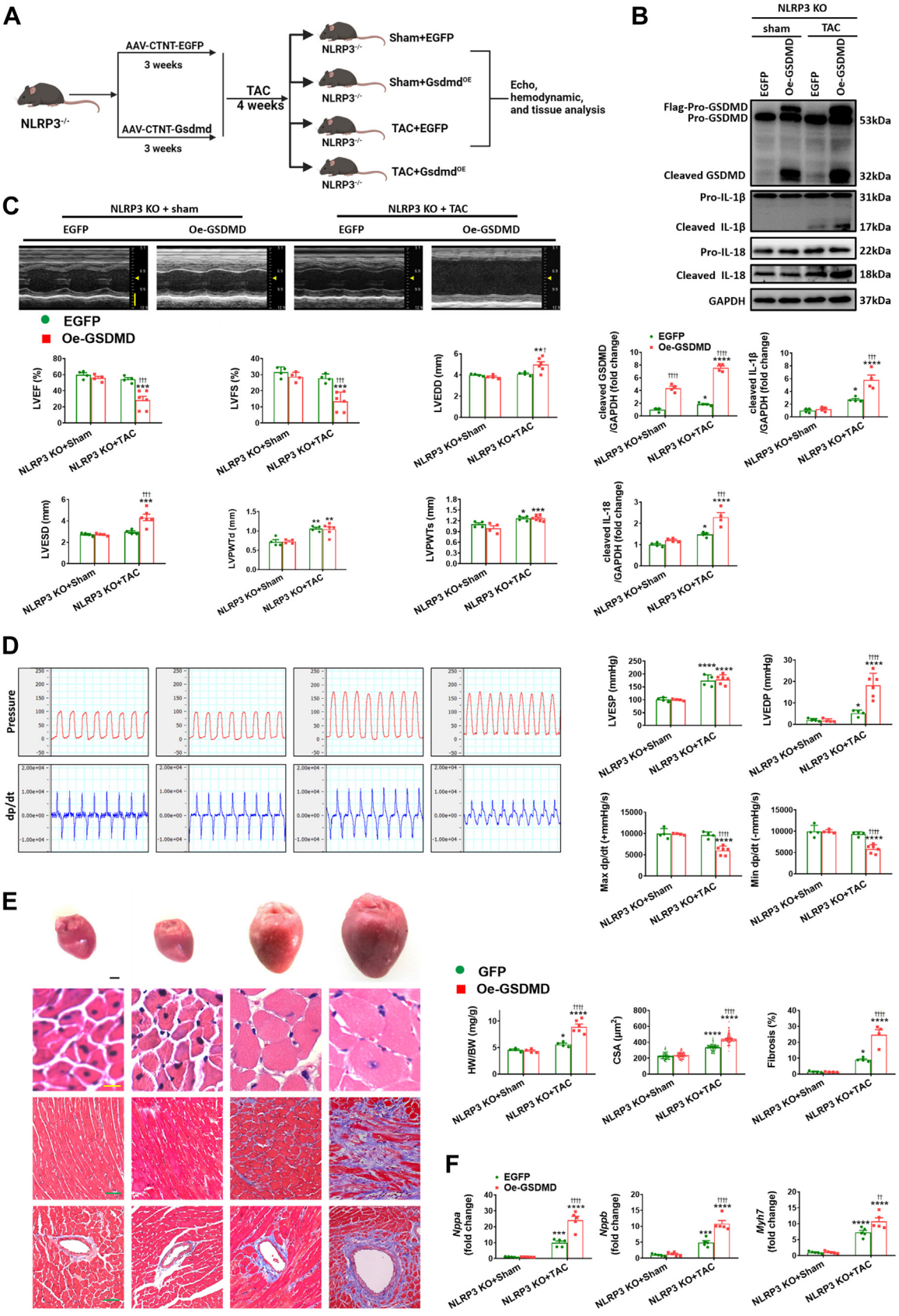

Continued on the next page

intracellular hub molecule of the innate immunity and the proinflammatory signaling whose effects on cardiac hypertrophy remain controversial.[26,29,30,49,50] In this regard, we found that TAK1 is activated strongly at both 2 weeks and 4 weeks post-TAC in conjunction with NLRP3 activation (Supplemental Figure 11). Somewhat unexpectedly, TAK1 was even more activated in NLRP3 KO mice subjected to pressure overload compared with WT control mice at both time points (**Figure 4A**). Consistent with in vivo observations, administration of MCC950 increased the TAK1 activation in Ang II-treated NMVMs (**Figure 4B**). Collectively, our data show that TAK1 activation associated with hypertrophy induction is actually enhanced by interference with NLRP3 signaling.

To further explore how NLRP3 regulates TAK1, we performed bioinformatics analyses of using the STRING database and Cytoscape platform (**Figure 4C**), which revealed that NLRP3 interacts with a number of proteins involved in innate immunity and inflammation such as CASP1, NEK, PYCARD, and TAK1 (MAP3K7). Consistent with these observations, PRISM was used to identify interactions binding domains between TAK1 and NLRP3, which are predicted to have interaction energies of −24.57 kcal/mol (**Figure 4D**). Interactions between NLRP3 and TAK1 were verified by coimmunoprecipitation in NMVMs and cardiac tissue, the results establish that NLRP3 and TAK1 interact under steady-state conditions, which appears to be reduced following hypertrophy induction (with either Ang II stimulation or TAC) (**Figure 4E**, Supplemental Figure 12A). In addition, with the help of plasmids with murine HA-tagged WT NLRP3 and murine Flag-tagged WT TAK1 or the S412A mutation, we have determined that the binding between NLRP3 and TAK1 is independent on phosphorylation (Supplemental Figure 12B). Taken together, these results indicate that NLRP3 deficiency directly promotes TAK1 activation in pressure overload hearts.

TAK1 DEFICIENCY EXACERBATES CARDIAC HYPERTROPHY AND DYSFUNCTION IN BOTH WT AND NLRP3 KO MICE UNDER PRESSURE OVERLOAD. Considering that NLRP3 deficiency enhances TAK1 activation in hypertrophic hearts, we speculated that TAK1 may reduce adverse remodeling associated with hypertrophic stimuli. To test this notion, we generated mice cardiac-specific knockdown of TAK1 (shTAK1) through ultrasound-guided closed-chest intramyocardial injection of AAV9 carrying shTAK1. This approach indicated good efficiency of TAK1 knockdown in the heart (**Figures 5A to 5H**, Supplemental Figure 5C). At baseline, no significant cardiac structural and functional difference was found between the shTAK1 and shRNA control mice, either in WT mice or in NLRP3 KO mice (**Figures 5B and 5C**). In response to pressure overload, TAK1 deficiency exacerbates cardiac hypertrophy and dysfunction, not only in WT mice, but also in NLRP3 KO mice (**Figures 5B to 5G**, Supplemental Figure 13, Supplemental Table 7). In particular, cardiac remodeling was more conspicuous in WT mice, as evidenced by results of structure and function by echocardiographic and invasive hemodynamic measure, cardiac hypertrophy and fibrosis by histological evaluation, and reprogramming of fetal genes by quantitative PCR assessment (**Figures 5B to 5G**, Supplemental Figure 13, Supplemental Table 7). NMVMs were then transfected with adenovirus harboring TAK1 shRNA to establish TAK1 knockdown (Ad-shTAK1) cell models before the Ang II challenge (Supplemental Figure 6C). Consistent with the in vivo results, Ad-shTAK1 induced remarkable increases in the size of NMVMs and up-regulation of fetal genes of NMVMs

FIGURE 3 Continued

(A) In vivo experimental overall schematic to explore the effects of cardiac GSDMD overexpression in NLRP3 KO mice subjected to TAC. Male NLRP3 KO mice were administered a tail vein injection of AAV9 vector carrying recombinant GSDMD, with the cTnT promoter. Vector virus AAV9-EGFP was used as negative control. 3 weeks later, these mice were subjected to TAC surgery or sham operation for 4 weeks, followed by echo, hemodynamic and tissue analysis. (B) Representative Western blot images and quantification showing the cleaved- and pro-forms of GSDMD, IL-1β, IL-18 in left ventricular samples from NLRP3 KO mice with AAV9-transfected GSDMD (Oe-GSDMD) or EGFP after 4 weeks of TAC or sham operation (n = 4 independent experiments). (C) Representative M-mode echocardiograms and quantification of left ventricle (n = 4 to 6 mice per group). Vertical scale bar, 2 mm, horizontal scale bar, 0.1 second. (D) Schematic presentations and quantification of left ventricular pressure, schematic presentations and quantification of left ventricular contraction velocity and relaxation velocity (n = 4 to 6 mice per group). Vertical scale bars, 100 mm Hg/s for pressure, 10,000 mm Hg/s for dp/dt; horizontal scale bar, 0.5 second for pressure and dp/dt. (E) Upper to lower, representative images of heart, cardiomyocytes stained by hematoxylin and eosin (scale bar, 20 μm), interstitial fibrosis stained by Masson's trichrome (scale bar, 50 μm), perivascular fibrosis stained by Masson's trichrome (scale bar, 50 μm), quantification of HW/BW, CSA of cardiomyocyte (n = 100 cells per group), and fibrotic ratio expressed as % area (n = 8 to 12 fields per group). (F) Real-time quantitative PCR analyses for the mRNA levels of atrial natriuretic peptide (*Nppa*), brain natriuretic peptide (*Nppb*), and beta-myosin heavy chain (*Myh7*) in left ventricular samples (n = 4 independent experiments). Mean ± SEM. *$P < 0.05$, **$P < 0.01$, ***$P < 0.001$, ****$P < 0.0001$ vs sham, †$P < 0.05$, ††$P < 0.01$, †††$P < 0.001$, ††††$P < 0.0001$ vs EGFP. Abbreviations as in **Figures 1 and 2**.

FIGURE 4 NLRP3 Deficiency Enhanced Activation of TAK1 in Hypertrophic Hearts

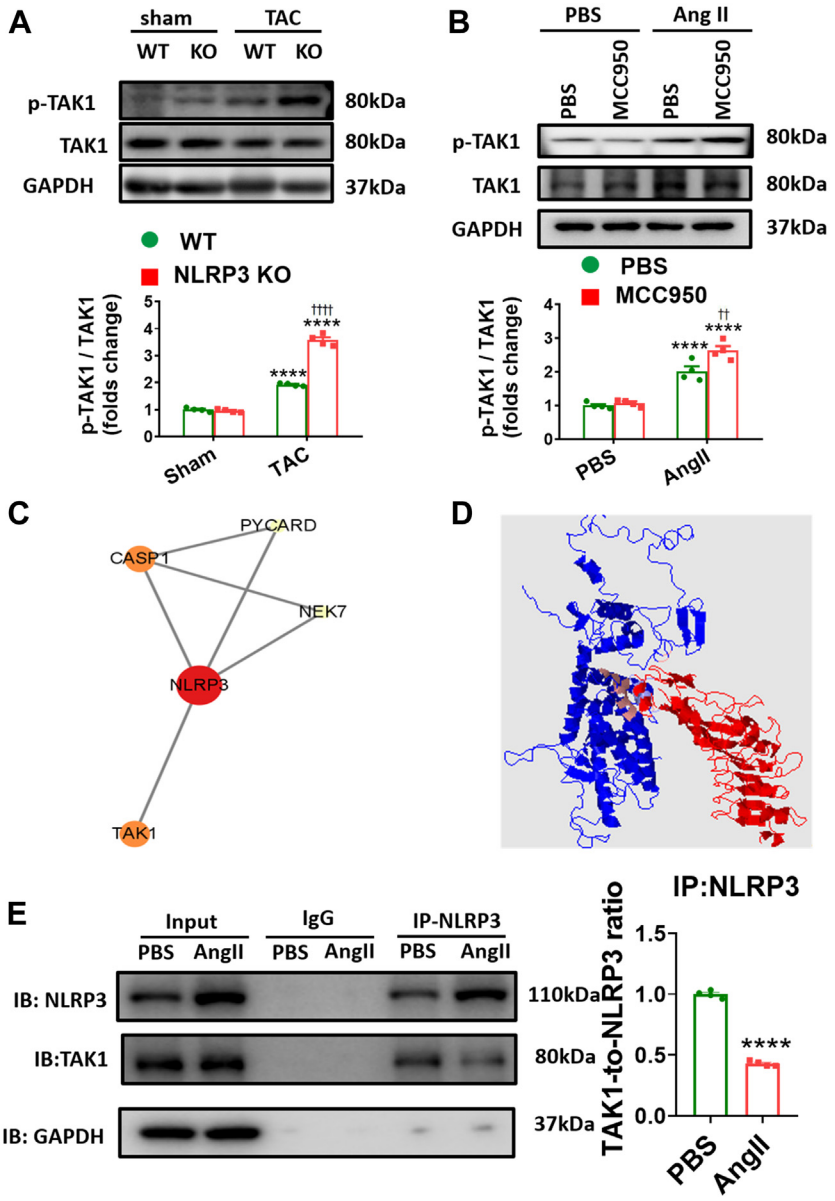

(A) Representative Western blot images and quantification showing phosphorylation levels of TAK1 in left ventricular samples from NLRP3 KO mice after 4 weeks of TAC or sham operation (n = 4 independent experiments). (B) Representative Western blot images and quantification showing phosphorylation levels of TAK1 from MCC950 incubated neonatal mouse ventricular myocytes (NMVMs) after treatment with Ang II or phosphate-buffered saline for 48 hours (n = 4 independent experiments). (C) String database identifies protein-protein interaction of NLRP3 and TAK1. (D) Structure-based interacting surface of NLRP3 (in red) and TAK1 (in blue) modeled by PRISM. The key interacting peptides are labeled in maroon. (E) Coimmunoprecipitation analysis and quantification of NLRP3 and TAK1 in NMVMs. Mean ± SEM. ****$P < 0.0001$ vs sham, ††††$P < 0.0001$ vs WT in A. ****$P < 0.0001$ vs PBS, ††$P < 0.01$ vs PBS+Ang II in B. ****$P < 0.0001$ vs PBS in E. Abbreviations as in Figure 1.

FIGURE 5 TAK1 Deficiency Aggravates Cardiac Remodeling in Both WT and NLRP3 KO Mice Under Pressure Overload

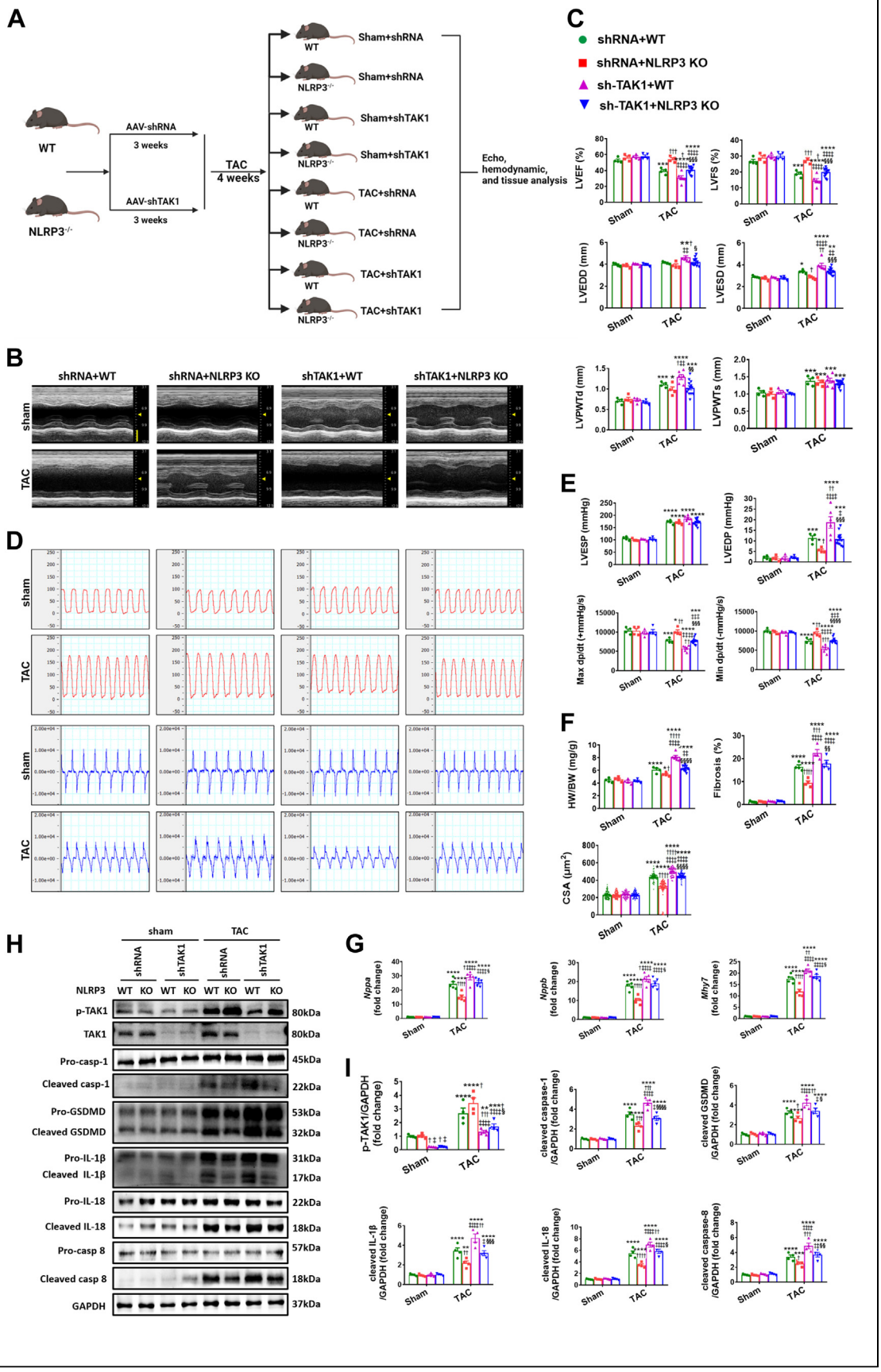

Continued on the next page

treated with Ang II, with or without MCC950 administration (Figures 6A and 6B).

We then sought to determine the function of TAK1 deficiency in pyroptosis. Under pressure overload, pyroptotic signals (cleavage of caspase-1, IL-18, IL-1β, and GSDMD) were up-regulated after shTAK1 treatment in both WT and NLRP3 KO mice, and in particular were more intensified in shTAK1+WT animals (Figures 5H and 5I). Moreover, considering TAK1 was recently reported to be involved in caspase-8-dependent cleavage of GSDMD through an alternative NLRP3 inflammasome pathway,[12,28] we also examined the changes in caspase-8 activation following TAK1 knockdown and found similar changes in caspase-8 activation as those observed in the aforementioned pyroptotic components (Figures 5H and 5I). In agreement with the in vivo results, shTAK1 aggravated pyroptosis in NMVMs challenged with Ang II, with or without cotreatment with MCC950 (Figures 6C and 6D, Supplemental Figure 4D). To further verify the role of TAK1 binding to NLRP3 in NLRP3 expression and in the pyroptosis-relevant inflammasome assembly and subsequent caspase-1 activation, we further investigated the effect of TAK1 knockdown on NLRP3 inflammasome assembly and found that the signaling of NLRP3, apoptosis-associated speck-like protein containing a caspase-recruitment domain (ASC), and caspase-1, which are important components of the NLRP3 inflammasome, were exacerbated after shTAK1 administration (Supplemental Figures 14 and 15). Taken together, cardiac-specific TAK1 knockdown exacerbates cardiac remodeling and pyroptosis in both WT and NLRP3 KO mice under pressure overload, indicative of a complex formed by NLRP3 and TAK1 to execute reciprocal inhibition.

DISCUSSION

It is established that NLRP3 activates caspase-1, which cleaves and activates GSDMD, as well as induces maturation of IL-1β and IL-18, making the NLRP3/caspase-1/GSDMD pathway critical in regulating pyroptosis.[12,14,15] NLRP3-initiated pyroptosis is increasingly recognized as a pathological factor contributing to ischemic cardiovascular disease. Several studies have recently reported that NLRP3 is activated by pressure overload induced by TAC,[18,23,51] and during the preparation of this paper, 2 studies concluded that pressure overload induces pyroptosis by NLRP3 or GSDMD activation and aggravates cardiac hypertrophy and dysfunction.[11,52] Our study confirms that pressure overload in mouse hearts leads to NLRP3 inflammasome activation in association with adverse hypertrophic remodeling characterized by impaired contractile function and cardiac fibrosis. Additionally, we establish that cultured NMVMs treated with the hypertrophic agent, Ang II, also develop marked hypertrophy combined with robust NLRP3 inflammasome activation. A clear mechanistic link between NLRP3 inflammasome activation and adverse response to pressure overload (or Ang II-induced hypertrophy) was demonstrated by the observation that NLRP3 deficiency preserves cardiac function with pressure overload by mitigating cardiac pyroptosis. On the other hand, either indirect enhancement of pyroptosis by overexpression of caspase-1 or direct pyroptosis augmentation using

FIGURE 5 Continued

(A) In vivo experimental overall schematic to explore the effects of cardiac TAK1 knockdown in WT and NLRP3 KO mice subjected to TAC. Male WT and NLRP3 KO mice were administered an ultrasound-guided closed-chest intramyocardial injection of AAV9 carrying small hairpin RNA against TAK1, in line with its corresponding negative control. Three weeks later, these mice were subjected to TAC surgery or sham operation for 4 weeks, followed by echo, hemodynamic, and tissue analysis. (B) Representative M-mode echocardiograms and quantification of left ventricle in WT or NLRP3 KO mice 4 weeks after TAC or sham operation, either with pretreatment of AAV9 transfected small hairpin RNA against TAK1 (shTAK1) or EGFP (n = 4 to 13 mice per group). Vertical scale bar, 2 mm, horizontal scale bar, 0.1 second. (C) Quantification of echocardiographic parameters in B. (D) Schematic presentations and quantification of left ventricular pressure, schematic presentations and quantification of left ventricular contraction velocity and relaxation velocity (n = 4 to 13 mice per group). Vertical scale bars, 100 mm Hg/s for pressure, 10,000 mm Hg/s for dp/dt; horizontal scale bar, 0.5 second for pressure and dp/dt. (E) Quantification of invasive hemodynamic parameters in D. (F) Quantification of HW/BW, CSA of cardiomyocyte (n = 100 cells per group), and fibrotic ratio expressed as % area (n = 8 to 26 fields per group). (G) Real-time quantitative PCR analyses for the mRNA levels of atrial natriuretic peptide (*Nppa*), brain natriuretic peptide (*Nppb*), and beta-myosin heavy chain (*Myh7*) in left ventricular samples (n = 4 independent experiments). (H) Representative Western blot images and quantification showing the phosphorylation and/or total protein levels of TAK1, cleaved- and pro-forms of caspase-1, GSDMD, IL-1β, IL-18, and caspase-18 in left ventricular samples (n = 4 independent experiments). (I) Quantification of parameters in H. Mean ± SEM. *$P < 0.05$, **$P < 0.01$, ***$P < 0.001$, ****$P < 0.0001$ vs corresponding sham, †$P < 0.05$, ††$P < 0.01$, †††$P < 0.001$, ††††$P < 0.0001$ vs shRNA+WT, ‡$P < 0.05$, ‡‡$P < 0.01$, ‡‡‡$P < 0.001$, ‡‡‡‡$P < 0.0001$ vs shRNA+NLRP3 KO, §$P < 0.05$, §§$P < 0.01$, §§§$P < 0.001$, §§§§$P < 0.0001$ vs shTAK1+WT. Abbreviations as in Figures 1 and 2.

FIGURE 6 TAK1 Deficiency Exacerbates Ang II-Induced Cardiomyocyte Hypertrophy Under PBS and MCC950 Treatment

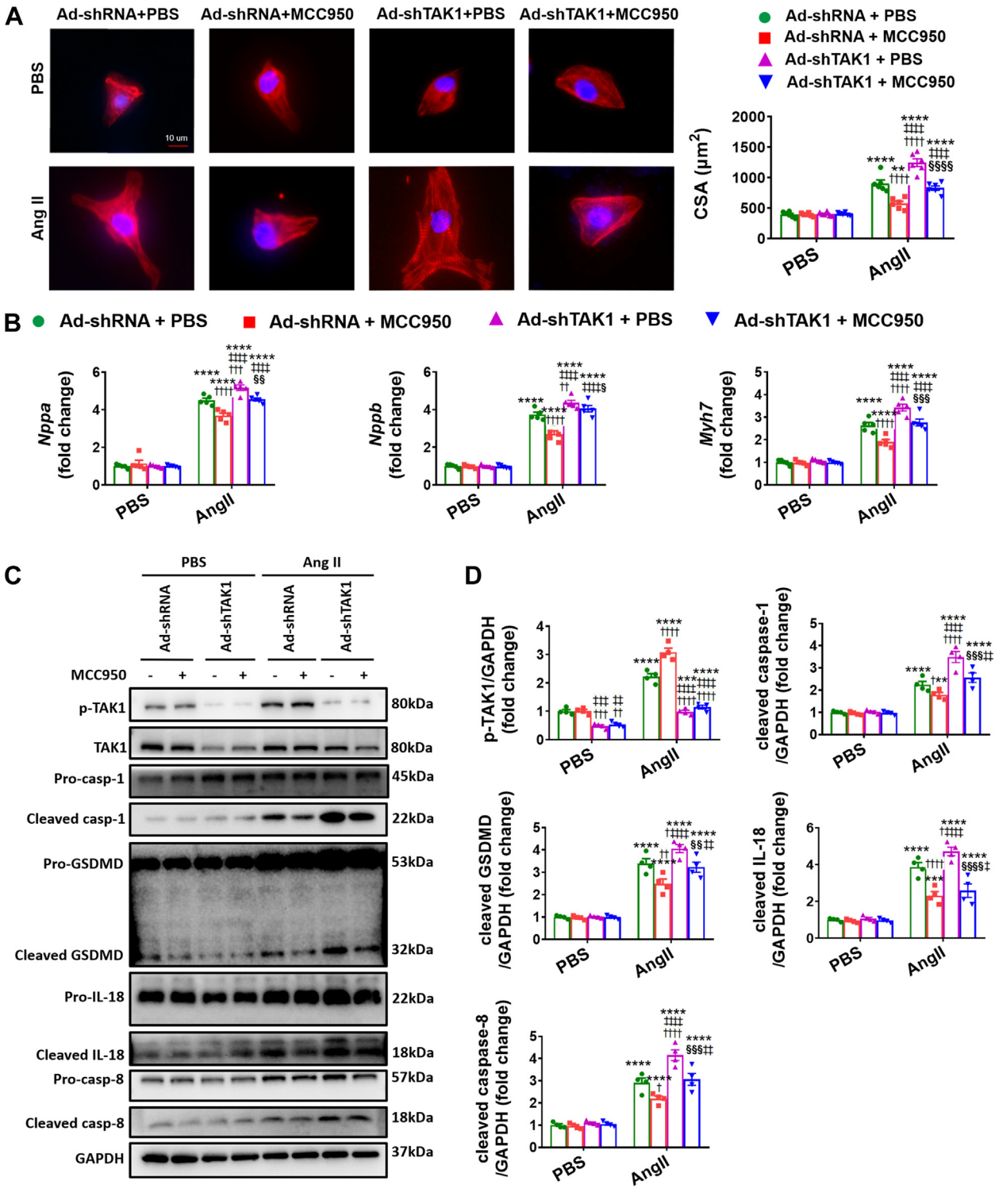

Continued on the next page

GSDMD overexpression abrogated the cardioprotection conferred either by NLRP3 deficiency in TAC mice or NLRP3 inhibition in Ang II-treated NMVMs. These findings support previous studies concluding that NLRP3-mediated pyroptosis plays a key role in adverse ventricular remodeling in response to hypertrophic stimuli.

Direct involvement of pyroptosis in mediating the adverse effects of TAC in mice and Ang II in cultured NMVMs was uncovered by overexpressing caspase-1 and GSDMD in the myocardium of NLRP3-deleted mice, which aggravated both pyroptosis cardiac remodeling. Therefore, each component of the NLRP3/caspase-1/GSDMD pyroptotic axis is crucial in the adverse cardiac remodeling induced by pressure overload. It is also worth mentioning that in our study, the detrimental effect exerted by cleavage of exogenous caspase-1 and GSDMD under pressure overload in the absence of NLRP3 was associated with the activation of other NLR family members such as NLRP1 or NLRC4, which can also activate caspase-1.[12,45,46] Indeed, we observed up-regulation of both NLRP1 and NLRC4 in WT and NLRP3 KO mice following pressure overload in relative to sham-operated mice. Although these findings appear to contradict a recent study concluding that the noncanonical inflammasome pathway (ie, caspase-11/GSDMD) is the main pathway triggering pyroptosis in cardiomyocytes following hypoxia/reoxygenation stress,[14] it seems likely that pressure overload-induced inflammatory response is distinct from those triggered by ischemic/hypoxia conditions.[18,21] Consistently, other studies have found prominent caspase-1 activation in cardiomyocytes isolated from pressure overload mice or administered with isoproterenol (another cardiomyocyte hypertrophy model), also suggesting crucial roles of NLRP3/caspase-1/GSDMD mediated pyroptosis in nonischemic heart disease.[18,44]

An intriguing finding in our studies was the observation that NLRP3 deficiency enhanced the extent of TAK1 activation seen with pressure overload in mouse hearts or treatment with the hypertrophic agent Ang II. This observation is consistent with previous studies demonstrating an interdependence between TAK1 and NLRP3 activation in other diseases.[27] Moreover, TAK1 has been reported to maintain myocardial homeostasis by preventing TNF-dependent necroptosis[26] while also protecting against cell death by suppressing GSDMD cleavage, pyroptosis, and inflammasome activation.[28] Thus, we considered the possibility that some of the benefits derived from NLRP3 inhibition in our hypertrophic models might be mediated by TAK1 activation. Indeed, shRNA-mediated knockdown of TAK1 diminished the benefit provided both by NLRP3 deficiency in TAC hearts as well as by NLRP3 blockade in Ang II-treated NMVMs. The functional interactions between TAK1 and NLRP3 might involve direct physical interactions because molecular modeling experiments in our study identified interactions domains on these proteins that are predicted to lead to energy stabilization. Direct interaction between the NLRP3 and TAK1 was supported by coimmunoprecipitation studies under steady-state conditions in mouse hearts, which also revealed marked negative modulation of this interaction by hypertrophic signaling (Ang II stimulation and TAC model). Thus, it is not unreasonable to suggest that NLRP3 and TAK1 potentially form a complex to inhibit one another. Although the functional consequences of their interaction may involve many molecules and pathways, such NLRP1 and NLRC4, not directly examined in our studies. In this regard, it is worth noting that in WT mice, NLRP3 expression and TAK1 activation were more remarkably aggravated at 2 weeks postoperative relative to 4 weeks (Supplemental Figure 11).

The dual role of TAK1 in cardiomyocyte pyroptosis and hypertrophic growth indicated by our results can help to explain some of the apparent contradictory findings of previous studies. For example, Zhang et al[29] demonstrated that extensive expression of TAK1 in neonatal mice resulted in hypertrophic cardiomyopathy, cardiac dysfunction, and premature

FIGURE 6 Continued

(A) Representative immunostaining images and quantification of NMVMs transfected with adenovirus harboring TAK1 (Ad-shTAK1) or with adenovirus containing EGFP (Ad-shRNA), treated with angiotensin II (Ang II, 1 μmol/L) or PBS for 48 hours, incubated with or without MCC950 (10 μmol/L) for 48 hours, followed by double staining of cardiac troponin T (cTnT, red) and 4′-6-diamidino-2-phenylindole (DAPI, blue). Scale bar, 10 μm (n = 100 cells per group). (B) Real-time quantitative PCR analyses for the mRNA levels of *Nppa*, *Nppb*, and *Myh7* in NMVMs (n = 4 independent experiments). (C) Representative Western blot images and (D) quantification showing the phosphorylation and/or total protein levels of TAK1, the cleaved- and pro-forms of caspase-1, GSDMD, IL-18, and caspase-18 in NMVMs (n = 4 independent experiments). Mean ± SEM. *$P < 0.05$, **$P < 0.01$, ***$P < 0.001$, ****$P < 0.0001$ vs corresponding PBS, †$P < 0.05$, ††$P < 0.01$, †††$P < 0.001$, ††††$P < 0.0001$ vs Ad-shRNA+PBS, ‡$P < 0.05$, ‡‡$P < 0.01$, ‡‡‡$P < 0.001$, ‡‡‡‡$P < 0.0001$ vs Ad-shRNA+MCC950, §$P < 0.05$, §§$P < 0.01$, §§§$P < 0.001$, §§§§$P < 0.0001$ vs Ad-shTAK1+PBS. Abbreviations as in Figures 1, 2, and 4.

death. On the contrary, Li et al[26] showed that adult-onset inducible hyperactivation of TAK1 prevented myocyte death and protected the heart against chronic pressure overload. Intriguingly, TAK1 is enriched in the embryonic and neonatal myocardium, down-regulated in the adult heart, up-regulated during compensated cardiac hypertrophy, and down-regulated again in heart failure.[29,49] Correspondingly, it has been recently found that early inhibition of CaMKII (a NLRP3 activator) and NLRP3 signaling in the first 1 or 2 weeks after TAC attenuates cardiac remodeling, but late inhibition of CaMKII and NLRP3 after 2 weeks did not.[18] In addition, our preliminary data showed that cardiac-specific overexpression of TAK1, through tail vein injection of AAV9 carrying TAK1 with the cTnT promotor, marginally affects cardiac hypertrophy in WT mice (data not shown). Therefore, the timing and extent of TAK1 activation may be critical in performing its dual role in cardiac homeostasis and its synergistic effects with NLRP3. This notion may explain why in the current study the cardiomyocyte size was smaller in NLRP3 KO mice than that in WT mice, but the LV wall thickness was comparable, for the NLRP3 KO mice experienced less cardiac pyroptosis than WT mice. It may also help answer why the inhibition of NLRP3 showed adverse effects in the heart in response to pressure overload,[23,24] considering those studies examined LV function 6 weeks (prominent heart failure) or 2 weeks (compensated cardiac function) after TAC, not at a timepoint of 4 weeks (transition period).

STUDY LIMITATIONS. Global deletion of NLRP3 may affect the systemic immune response during 4 weeks of TAC, and a cardiac-specific knockout murine model would be more specific to interpret the role of NLRP3 in mice exposed to pressure overload. Although further intensification of TAK1 signaling would be of interest to determine whether TAK1 overexpression protects against TAC-induced heart failure in WT mice, and our plans to conduct this as an independent study are warranted, a large amount of work would be required, considering the efforts in constructing cardiomyocyte-specific TAK1 overexpression mice and comprehensive evaluation of geometric and functional properties of them weeks after TAC operation.

CONCLUSIONS

Taken together, our study suggests that the NLRP3/caspase-1/GSDMD-mediated pyroptosis contributes to cardiac hypertrophy induced by pressure overload. NLRP3 deficiency exerts salutary effects by activation of TAK1 in response to pressure overload, whereas knockdown of TAK1 expression abolishes the cardioprotection of NLRP3 deficiency. The fine tuning of cardiomyocyte death and hypertrophic growth linking NLRP3 and TAK1 advances our understanding of the mechanism and therapeutic strategy of cardiac hypertrophy and heart failure.

ACKNOWLEDGMENTS The authors appreciate Jianguo Jia, Chunjie Yang, Bingyu Li, Sanli Qian, and Zhenzhong Zhang, from Shanghai Institute of Cardiovascular Diseases, Zhongshan Hospital, for their kindness with technical expertise. The authors also thank Guoping Zhang for his assistance in lab management.

FUNDING SUPPORT AND AUTHOR DISCLOSURES

This work was supported by the National Natural Science Foundation of China grants 81941002 (Dr Zou), 82170389 (Dr Wu), 82170255 (Dr S. Wang), 81730009 (Dr Zou), 81770274 (Dr S. Wang), 81670228 (Dr Wu), and 81500191 (Dr You), Laboratory Animal Science Foundation of Science and Technology Commission of Shanghai Municipality grants 201409004300 (Dr Zou) and 21140904400 (Dr Wu), Health Science and Technology Project of Shanghai Pudong New Area Health Commission grant PW2019A-13 (Dr You), and "Rising Sun" Excellent Young Medical Talents Program of Shanghai East Hospital grant 2019xrrcjh03 (Dr You). The authors have reported that they have no relationships relevant to the contents of this paper to disclose.

ADDRESS FOR CORRESPONDENCE: Prof Jian Wu OR Prof Yunzeng Zou, Shanghai Institute of Cardiovascular Diseases, Zhongshan Hospital and Institutes of Biomedical Sciences, Fudan University, 180 Feng Lin Road, Shanghai 200032, China. E-mail: wu.jian@zs-hospital.sh.cn OR zou.yunzeng@zs-hospital.sh.cn.

PERSPECTIVES

COMPETENCY IN MEDICAL KNOWLEDGE: This study presents a comprehensive view of the detrimental role of NLRP3/caspase-1/GSDMD-mediated pyroptosis in cardiac hypertrophy under pressure overload, through direct or indirect enhancement of pyroptosis. NLRP3 deficiency exerts salutary effects by activation of TAK1, whereas knockdown of TAK1 expression abolishes the cardioprotection of NLRP3 deficiency in hypertrophic hearts.

TRANSLATIONAL OUTLOOK: Future studies are warranted to determine the potential therapeutic benefit of TAK1-NLRP3 intervention, especially by ameliorating selective components of pyroptosis, in cardiomyocytes for the prevention and treatment of heart failure in patients with hypertension. This study also presents a translational strategy that antagonist against inflammation-induced cell death might be exploited therapeutically in other inflammatory and mechanical overload disorders, such as myocardial infarction and mitral regurgitation.

REFERENCES

1. Heidenreich PA, Bozkurt B, Aguilar D, et al. 2022 AHA/ACC/HFSA guideline for the management of heart failure: executive summary: a report of the American College of Cardiology/American Heart Association Joint Committee on Clinical Practice Guidelines. *J Am Coll Cardiol*. 2022;79(17):e263–e421.

2. Zou Y, Akazawa H, Qin Y, et al. Mechanical stress activates angiotensin II type 1 receptor without the involvement of angiotensin II. *Nat Cell Biol*. 2004;6:499–506.

3. Wu J, You J, Wang S, Zhang L, Gong H, Zou Y. Insights into the activation and inhibition of angiotensin II type 1 receptor in the mechanically loaded heart. *Circ J*. 2014;78:1283–1289.

4. Lin HB, Naito K, Oh Y, et al. Innate immune Nod1/RIP2 signaling is essential for cardiac hypertrophy but requires mitochondrial antiviral signaling protein for signal transductions and energy balance. *Circulation*. 2020;142:2240–2258.

5. Suetomi T, Miyamoto S, Brown JH. Inflammation in nonischemic heart disease: initiation by cardiomyocyte CaMKII and NLRP3 inflammasome signaling. *Am J Physiol Heart Circ Physiol*. 2019;317:H877–H890.

6. Liu X, Shi GP, Guo J. Innate immune cells in pressure overload-induced cardiac hypertrophy and remodeling. *Front Cell Dev Biol*. 2021;9:659666.

7. Chen GY, Nunez G. Sterile inflammation: sensing and reacting to damage. *Nat Rev Immunol*. 2010;10:826–837.

8. Zhang Y, Zhang XJ, Wang PX, Zhang P, Li H. Reprogramming innate immune signaling in cardiometabolic disease. *Hypertension*. 2017;69:747–760.

9. Chen A, Chen Z, Xia Y, et al. Liraglutide attenuates NLRP3 inflammasome-dependent pyroptosis via regulating SIRT1/NOX4/ROS pathway in H9c2 cells. *Biochem Biophys Res Commun*. 2018;499:267–272.

10. Ren J, Pei Z, Chen X, et al. Inhibition of CYP2E1 attenuates myocardial dysfunction in a murine model of insulin resistance through NLRP3-mediated regulation of mitophagy. *Biochem Biophys Acta Mol Basis Dis*. 2019;1865:206–217.

11. Yue R, Zheng Z, Luo Y, et al. NLRP3-mediated pyroptosis aggravates pressure overload-induced cardiac hypertrophy, fibrosis, and dysfunction in mice: cardioprotective role of irisin. *Cell Death Discov*. 2021;7(1):50. https://doi.org/10.1038/s41420-021-00434-y

12. Kelley N, Jeltema D, Duan Y, He Y. The NLRP3 inflammasome: an overview of mechanisms of activation and regulation. *Int J Mol Sci*. 2019;20(13):3328. https://doi.org/10.3390/ijms20133328

13. He WT, Wan H, Hu L, et al. Gasdermin D is an executor of pyroptosis and required for interleukin-1beta secretion. *Cell Res*. 2015;25:1285–1298.

14. Shi H, Gao Y, Dong Z, et al. GSDMD-mediated cardiomyocyte pyroptosis promotes myocardial I/R injury. *Circ Res*. 2021;129:383–396.

15. Jiang K, Tu Z, Chen K, et al. Gasdermin D inhibition confers antineutrophil-mediated cardioprotection in acute myocardial infarction. *J Clin Invest*. 2022;132(1):e151268. https://doi.org/10.1172/JCI151268

16. Gao Y, Shi H, Dong Z, Zhang F, Sun A, Ge J. Current knowledge of pyroptosis in heart diseases. *J Mol Cell Cardiol*. 2022;171:81–89.

17. Zhang KZ, Shen XY, Wang M, et al. Retinol-binding protein 4 promotes cardiac injury after myocardial infarction via inducing cardiomyocyte pyroptosis through an interaction with NLRP 3. *J Am Heart Assoc*. 2021;10:e022011.

18. Suetomi T, Willeford A, Brand CS, et al. Inflammation and NLRP3 inflammasome activation initiated in response to pressure overload by Ca(2+)/calmodulin-dependent protein kinase II delta signaling in cardiomyocytes are essential for adverse cardiac remodeling. *Circulation*. 2018;138:2530–2544.

19. Wu J, Dong E, Zhang Y, Xiao H. The role of the inflammasome in heart failure. *Front Physiol*. 2021;12:709703. https://doi.org/10.3389/fphys.2021.709703

20. Everett BM, Cornel JH, Lainscak M, et al. Anti-inflammatory therapy with canakinumab for the prevention of hospitalization for heart failure. *Circulation*. 2019;139:1289–1299.

21. Zeng C, Duan F, Hu J, et al. NLRP3 inflammasome-mediated pyroptosis contributes to the pathogenesis of non-ischemic dilated cardiomyopathy. *Redox Biol*. 2020;34:101523.

22. Qiu Z, Lei S, Zhao B, et al. NLRP3 inflammasome activation-mediated pyroptosis aggravates myocardial ischemia/reperfusion injury in diabetic rats. *Oxid Med Cell Longev*. 2017;2017:9743280.

23. Li F, Zhang H, Yang L, et al. NLRP3 deficiency accelerates pressure overload-induced cardiac remodeling via increased TLR4 expression. *J Mol Med*. 2018;96:1189–1202.

24. Higashikuni Y, Liu W, Numata G, et al. NLRP3 inflammasome activation through heart-brain interaction initiates cardiac inflammation and hypertrophy during pressure overload. *Circulation*. 2023;147(4):338–355.

25. Sandanger O, Gao E, Ranheim T, et al. NLRP3 inflammasome activation during myocardial ischemia reperfusion is cardioprotective. *Biochem Biophys Res Commun*. 2016;469:1012–1020.

26. Li L, Chen Y, Doan J, Murray J, Molkentin JD, Liu Q. Transforming growth factor beta-activated kinase 1 signaling pathway critically regulates myocardial survival and remodeling. *Circulation*. 2014;130:2162–2172.

27. Malireddi RKS, Gurung P, Mavuluri J, et al. TAK1 restricts spontaneous NLRP3 activation and cell death to control myeloid proliferation. *J Exp Med*. 2018;215:1023–1034.

28. Orning P, Weng D, Starheim K, et al. Pathogen blockade of TAK1 triggers caspase-8-dependent cleavage of gasdermin D and cell death. *Science*. 2018;362:1064–1069.

29. Zhang D, Gaussin V, Taffet GE, et al. TAK1 is activated in the myocardium after pressure overload and is sufficient to provoke heart failure in transgenic mice. *Nat Med*. 2000;6:556–563.

30. He B, Zhao YC, Gao LC, et al. Ubiquitin-specific protease 4 is an endogenous negative regulator of pathological cardiac hypertrophy. *Hypertension*. 2016;67:1237–1248.

31. You J, Wu J, Zhang Q, et al. Differential cardiac hypertrophy and signaling pathways in pressure versus volume overload. *Am J Physiol Heart Circ Physiol*. 2018;314:H552–H562.

32. Huang J, Wu J, Wang S, et al. Ultrasound biomicroscopy validation of a murine model of cardiac hypertrophic preconditioning: comparison with a hemodynamic assessment. *Am J Physiol Heart Circ Physiol*. 2017;313:H138–H148.

33. Wu J, Bu L, Gong H, et al. Effects of heart rate and anesthetic timing on high-resolution echocardiographic assessment under isoflurane anesthesia in mice. *J Ultrasound Med*. 2010;29:1771–1778.

34. Wu J, You J, Wang X, et al. Left ventricular response in the transition from hypertrophy to failure recapitulates distinct roles of Akt, β-arrestin-2, and CaMKII in mice with aortic regurgitation. *Ann Transl Med*. 2020;8:219–237.

35. Dai F, Li X, Li X, et al. Caspase-1 abrogates the salutary effects of hypertrophic preconditioning in pressure overload hearts via IL-1β and IL-18. *Front Mol Biosci*. 2021;8:641585. https://doi.org/10.3389/fmolb.2021.641585

36. Li X, Tan W, Zheng S, et al. Differential mRNA expression and circular RNA-based competitive endogenous RNA networks in the three stages of heart failure in transverse aortic constriction mice. *Front Physiol*. 2022;13:777284.

37. Lin H, Zhu Y, Zheng C, et al. Antihypertrophic memory after regression of exercise-induced physiological myocardial hypertrophy is mediated by the long noncoding RNA Mhrt779. *Circulation*. 2021;143:2277–2292.

38. Wu J, Lu J, Huang J, et al. Variations in energy metabolism precede alterations in cardiac structure and function in hypertrophic preconditioning. *Front Cardiovasc Med*. 2020;7:602100.

39. Huang C, Sharma A, Thakur R, et al. Asporin, an extracellular matrix protein, is a beneficial regulator of cardiac remodeling. *Matrix Biol*. 2022;110:40–59.

40. Doncheva NT, Morris JH, Gorodkin J, Jensen LJ. Cytoscape StringApp: network analysis and visualization of proteomics data. *J Proteome Res*. 2019;18:623–632.

41. Ren J, Sun M, Zhou H, et al. FUNDC1 interacts with FBXL2 to govern mitochondrial integrity and cardiac function through an IP3R3-dependent manner in obesity. *Sci Adv*. 2020;6:eabc8561.

42. Li X, Dai F, Wang H, et al. PCSK9 participates in oxidized-low density lipoprotein-induced myocardial injury through mitochondrial oxidative stress and Drp1-mediated mitochondrial fission. *Clin Transl Med*. 2022;12:e729.

43. Toldo S, Abbate A. The NLRP3 inflammasome in acute myocardial infarction. *Nat Rev Cardiol*. 2018;15:203–214.

44. Xiao H, Li H, Wang JJ, et al. IL-18 cleavage triggers cardiac inflammation and fibrosis upon beta-adrenergic insult. *Eur Heart J*. 2018;39:60–69.

45. Kaushal V, Dye R, Pakavathkumar P, et al. Neuronal NLRP1 inflammasome activation of Caspase-1 coordinately regulates inflammatory interleukin-1-beta production and axonal degeneration-associated Caspase-6 activation. *Cell Death Differ*. 2015;22:1676–1686.

46. Zhang P, Liu Y, Hu L, et al. NLRC4 inflammasome-dependent cell death occurs by a complementary series of three death pathways and determines lethality in mice. *Sci Adv*. 2021;7:eabi9471.

47. Shimizu I, Minamino T. Physiological and pathological cardiac hypertrophy. *J Mol Cell Cardiol*. 2016;97:245–262.

48. Su F, Zhao L, Zhang S, et al. Cardioprotection by PI3K-mediated signaling is required for anti-arrhythmia and myocardial repair in response to ischemic preconditioning in infarcted pig hearts. *Lab Invest*. 2015;95:860–871.

49. Li L, Chen Y, Li J, et al. TAK1 regulates myocardial response to pathological stress via NFAT, NFkappaB, and Bnip3 pathways. *Sci Rep*. 2015;5:16626.

50. Yuan L, Bu S, Du M, et al. RNF207 exacerbates pathological cardiac hypertrophy via post-translational modification of TAB1. *Cardiovasc Res*. 2023;119(1):183–194.

51. Yao C, Veleva T, Scott L Jr, et al. Enhanced cardiomyocyte NLRP3 inflammasome signaling promotes atrial fibrillation. *Circulation*. 2018;138:2227–2242.

52. Han J, Dai S, Zhong L, et al. GSDMD (gasdermin D) mediates pathological cardiac hypertrophy and generates a feed-forward amplification cascade via mitochondria-STING (stimulator of interferon genes) axis. *Hypertension*. 2022;79(11):2505–2518.

KEY WORDS **cardiac remodeling, cell death, hypertrophy, pressure overload, pyroptosis**

APPENDIX **For supplemental figures and tables, please see the online version of this paper.**